SCIENTIFIC REPORTS

OPEN

SUBJECT AREAS:
CERAMICS
NANOWIRES

Received
9 April 2014

Accepted
9 October 2014

Published
30 October 2014

Correspondence and requests for materials should be addressed to B.J.L. (stslbj@outlook.com) or C.X.W. (wchengx@mail.sysu.edu.cn)

Si-Doped Ceramic Al_4O_4C Nanowires: Full-Color Emission and Optical Waveguide Behavior

Y. Sun, H. X. Lei, H. Cui, G. W. Yang, B. J. Li & C. X. Wang

State key laboratory of optoelectronic materials and technologies, School of Physics Science and Engineering, Sun Yat-sen (Zhongshan) University, Guangzhou 510275, People's Republic of China

The increasing prosperity of the photonics field has hastened the development of several sub-disciplines, with the aim to create advanced photonic devices, produce photonic circuits and eventually enable all-optical communication. This development has resulted in the demand for micro-nano-sized functional units with specific space dimensions (1D & 2D) for subwavelength photon operation purposes. The fundamental task involves a search for available semiconductor materials as micro-nano light sources and optical interconnections; in this regard, finding a white-light source is the most challenging task because typical band-band emission is not possible in the single phase. Using current approaches, which rely on surface-state emission and the integration of various emission components, it is impossible to achieve single-phase, single-unit components with specific space dimensions. Here, we achieved continuous full-color (ultraviolet to red) emission by engineering a single Al_4O_4C nanowire with Si doping, which created impurity levels in the bandgap and conduction band. High light propagation performance was also observed when blue, green and red lasers were coupled into a single nanowire using a tapered optical fiber. This novel 1D nanostructure is an excellent candidate for use in future photonic circuits as a white-light source or interconnection component.

Recently, subwavelength photonic integration devices based on nanowires/nanofibers have been comprehensively investigated for use as optical diodes, logic gates and other functional components for future optical computers and eventually all-optical communication, relying on their natural 1D features and advantageous photonic properties, such as their optical waveguide and micro-nano laser source capabilities[1–2]. In general, suitable micro-nano materials with advanced optical waveguide and light source functionalities are critical to producing functional devices. Special materials and structures are often required based on specific functionalities, which presents a challenge to nanomaterial scientists. For example, the design of a white-light source in a 1D configuration poses a great challenge[3–8]. First, simple band-band emission in a single semiconductor micro-nano unit is not possible because of the band edge emission characteristic. Second, it is difficult to achieve white emission in 1D homogeneous structures in a simple manner using common approaches such as doping an active host material with several types of fluorescent dyes or designing semiconductor nanocrystals with various sizes and composites (relying on surface-state and mixed multi-spectral emission)[9–15].

Therefore, an approach for achieving low-dimensional micro-nano white-light sources for application in photonic integration circuits is greatly desired[16–21]. Ideally, a multi-color optical waveguide property would also be simultaneously achieved. Here, we report an important achievement based on previous work, in which we designed 1D tapered Al_4O_4C ceramics via the VLS (vapor-liquid-solid) process as a new type of blue-light emitter[22]. Here, we engineered the electronic structure of this material via Si atom doping, resulting in new levels in the fundamental bandgap and the conduction band, as revealed by CL (cathode luminescence) spectroscopy. A single Al_4O_4C nanowire with a Si dopant displayed full-color (ultraviolet to red) light emission behavior when excited by cathode electrons, which corresponds to white light in the CIE-1931 chromaticity diagram with a correlated color temperature of approximately 8000 K. When blue, green and red lasers were imported into the nanowire by coupling between a nanowire and a tapered optical fiber, excellent optical waveguide behavior was observed. Quantitative measurements indicate that the propagation efficiencies of a single nanowire with a length of approximately 50 μm were 80.9%, 85.3% and 91.2%. Therefore, Si-doped Al_4O_4C is a good candidate for use as a white-light source and as a waveguide interconnection for future photonic devices.

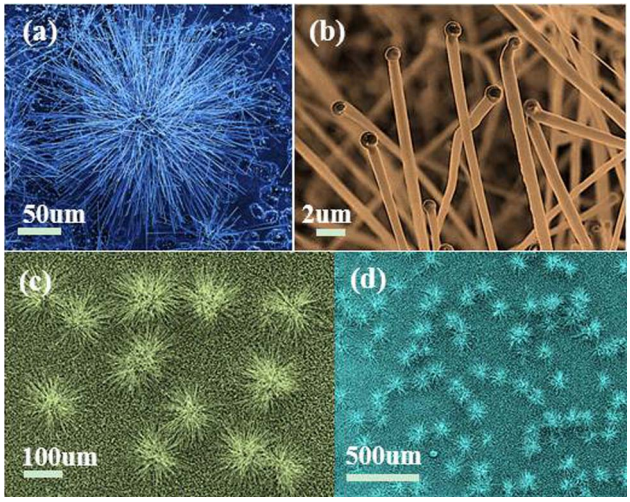

Figure 1 | SEM images of the product on the W substrate. (a) A single radical flower composed of nanowires, (b) a closer view of the nanowires, and (c) and (d) low-magnification images of several nanowire flowers distributed on the W substrate.

Results

Characterization of the Al_4O_4C:Si 1D nanostructures. Scanning electron microscopy (SEM) characterization reveals that hedgehog-like nanowire balls are distributed on the substrate. Upon closer inspection, most of the nanowires are observed to exhibit a gentle cone profile with a large aspect ratio. A typical nanowire is as long as 100 μm with a diameter of less than 1 μm. As shown in Fig. 1, some of the 1D structures exhibit a regular quadrangular prism shape, whereas others have one zigzag face. The as-prepared sample was analyzed using X-ray diffraction (XRD), from which signals corresponding to Al_4O_4C (PDF#48-1583), W_2C (PDF#65-3896), WC (PDF#65-4539) and W (PDF#04-0806) were detected, as displayed in Fig. 2(a). No distinguishable peak shift was observed; Al_4O_4C is the main product, and the W_2C and WC phases are the accompanying products due to carbonization of the W substrate, which has been described in detail elsewhere[23]. Further characterization using transmission electron microscopy (TEM) and Raman spectroscopy confirmed that all of the nanowires consisted of Si-doped Al_4O_4C.

We selected a single nanowire for the Raman spectroscopy investigation, as shown in Fig. 2(b). The blue curve represents the Raman spectrum of the pure Al_4O_4C needle[22], and the red curve represents

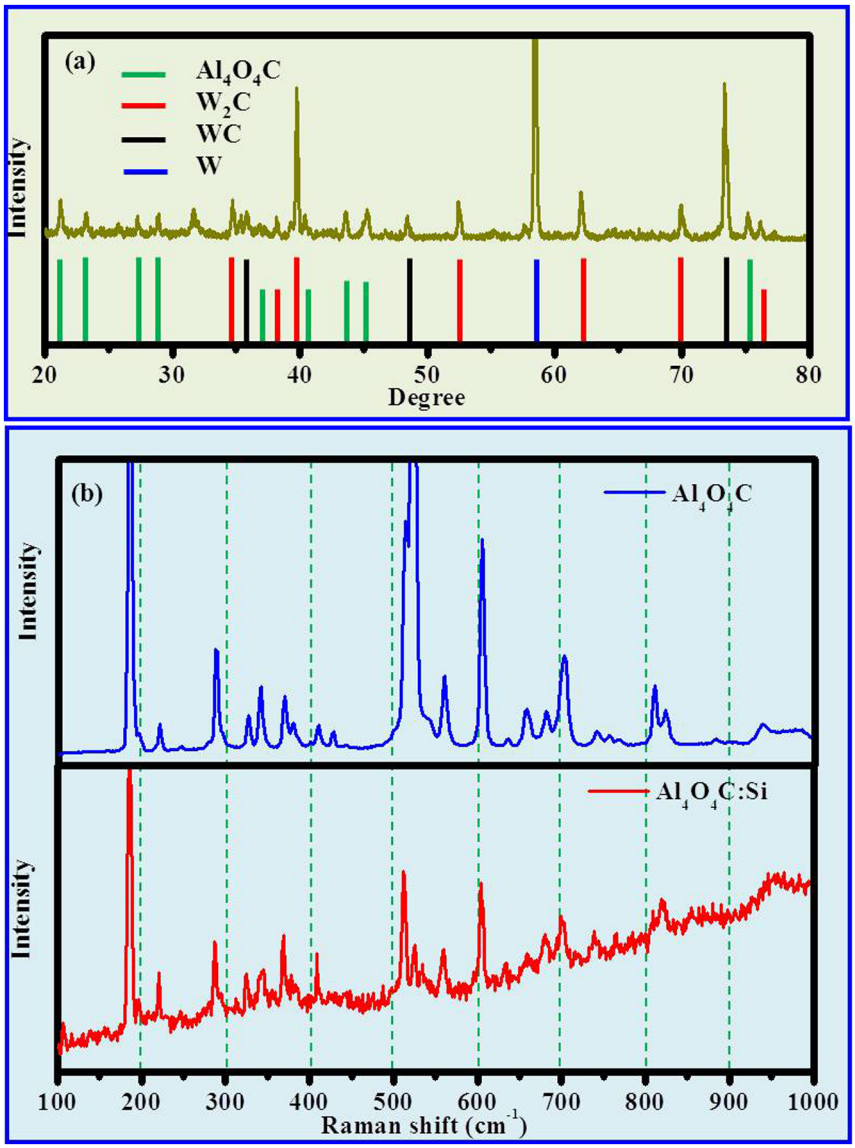

Figure 2 | Phase analysis of the sample: (a) XRD pattern and (b) Raman spectra of an Al_4O_4C micro-nano taper and a single Si-doped Al_4O_4C nanowire.

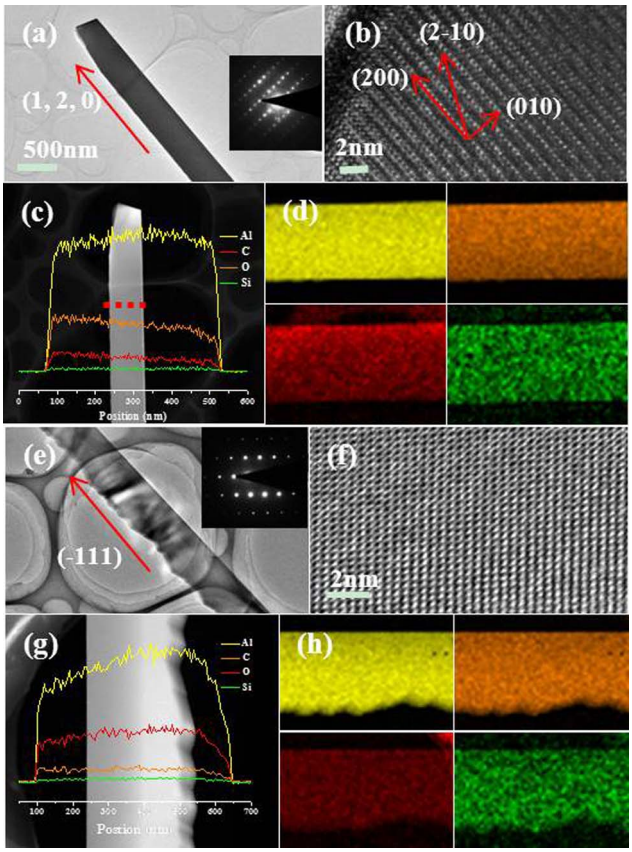

Figure 3 | TEM characterization of the structure and composition of two nanowires. (a) Low-magnification image of a single nanowire; the inset shows the corresponding SAED pattern; (b) HRTEM image of the nanowire from (a); (c) and (d) EDS line scans and mapping analysis of a single nanowire, which imply that Si atoms are distributed in the lattice; (e–h) characterization results of another nanowire with a zigzag profile, obtained using the same methods.

data from a single nanowire. A comparison of the spectra reveals that almost no shift occurs, confirming the presence of the Al_4O_4C phase. Subtle differences, such as the absence of several weak peaks compared with the blue curve, may originate from the thinner diameter and the presence of the Si dopant.

TEM can be used to perform elemental and structural analysis on a single nanostructure. Here, high-resolution TEM (HRTEM) and EDS mapping methods were employed, as shown in Fig. 3, and 1D nanostructures with different profiles were investigated. Figs. 3(a–d) present analytical results for a single nanostructure with a regular quadrangular prism shape, and Figs. 3(e–h) present results for a single irregular quadrangular prism nanostructure with one zigzag face. Notably, the nanowire with smooth facets has a thicker body. Selected area electron diffraction (SAED) patterns and HRTEM images confirmed that both of these structures have the same crystal lattice, orthorhombic Al_4O_4C. Further EDS line scanning and EDS mapping revealed that a certain proportion of Si atoms (~0.1% mol%) is included in the lattice. Based on the above characterization, we believe that the 1D nanostructures are Si-doped Al_4O_4C.

Discussion

To investigate the luminescence performance and the electronic structure, we applied cathode electrons to excite a single 1D nanostructure, utilizing its micro-domain analysis advantages. For units with different profiles, CL images were recorded, as shown in Fig. 4. Figs. 4(a) and (b) present SEM images of nanowires with different profiles, and Figs. 4(d) and (e) present corresponding CL images.

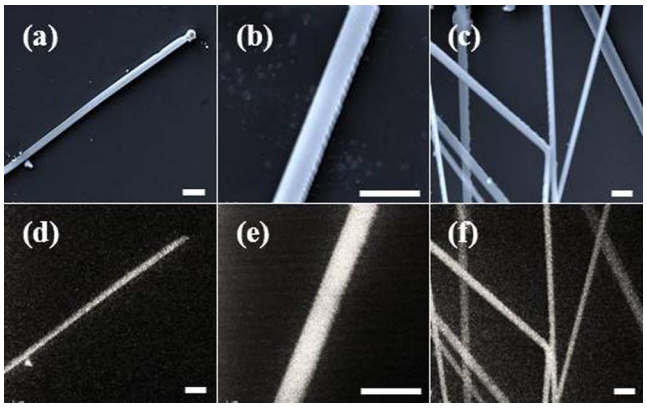

Figure 4 | CL investigation of the samples. (a–c) Three sets of nanowires selected for application of the CL test. (d), (e) and (f) CL images corresponding to (a), (b) and (c). The scale bars are 2 μm.

Fig. 4(f) shows a CL image of several nanostructures stacked together, as displayed in Fig. 4(c), for which all of the nanostructures exhibit the same light emission behavior. Additionally, the emission spectra were recorded to confirm the consistency among different units. As expected, all of the spectra exhibit the same profile, as illustrated in Fig. 5(a). The cathode-electron irradiation clearly yields light emission from the ultraviolet to red region. After adjusting the spectrum to the CIE 1931 chromaticity diagram, as shown in Fig. 5(b), the emission spectrum was determined to be in the CWF (cool white florence) region in the chromaticity diagram, with a CCT (correlated color temperature) of approximately 8000 K. The three vertices of the red triangle represent the coordinates of the pure green, red and blue light regions according to the National Television Systems Committee (NTSC). The red square at the coordinate of (0.33, 0.33) represents pure white light with a CCT of approximately 5600 K. The black triangle represents the coordinate of our spectrum, which is consistent with CWF in the industrial LED field. Fig. 5(c) presents the CL spectra of pure Al_4O_4C (red line) and the Si-doped phase (blue line), which display an obvious difference. Both of the emission spectra exhibit a similar peak corresponding to band-band transitions at 420 nm and 418 nm, respectively. There are two additional peaks in the Si-doped phase at 331 nm and 620 nm, which implies that the introduction of Si atoms results in several levels within the fundamental bandgap and even in the conduction band that are available for radiative transition. Based on the CL spectrum, we can use Fig. 5(d) to illustrate the possible transition process, as indicated by the colored dotted arrows.

The Si-doped Al_4O_4C nanowires display a broadened emission spectrum ranging from the ultraviolet to red region compared with pure Al_4O_4C needles. This broadening originates from the creation of impurity levels due to the introduction of Si atoms. According to the CL results, we believe that the new levels may be close to the bottom of the conduction band and may even penetrate into the conduction band, such that the emission spectrum is widened toward shorter wavelengths. In addition, the light emission behavior implies that a lower level is introduced. The significant dissimilarity between the light emission spectra of pure Al_4O_4C and Si-doped Al_4O_4C suggests that the photoelectric performance of Al_4O_4C can be tuned through doping and that other strategies may be used to design various types of Al_4O_4C-based materials with special photoelectric functionalities.

Achieving full-color emission from a single nanowire is a great breakthrough and may be advantageous if used as a white-light source in future photonic devices compared with present strategies such as complicated multi-phase composite materials and simple blends of various luminescence materials[23]. Furthermore, the multi-color light waveguide ability is a fundamental property for

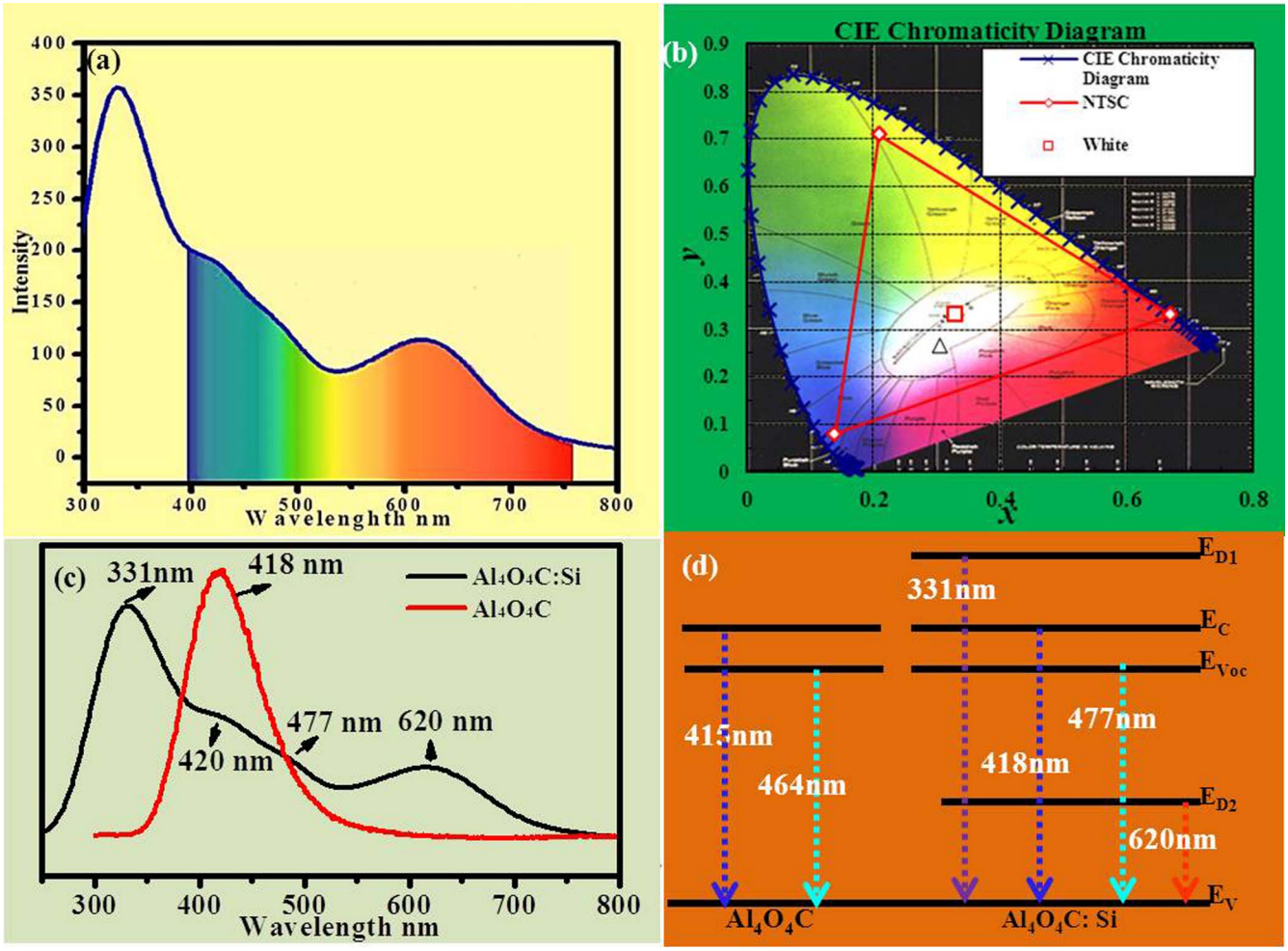

Figure 5 | CL spectrum analysis. (a) CL spectrum of the nanowires shown in Fig. 4(c), which illustrates full-color emission from the ultraviolet to infrared region. (b) Color temperature characterization and coordinate of the emission spectrum when adjusted in the chromaticity diagram 1931. (c) Comparison between the CL spectra of the Al_4O_4C micro-nano taper and Si-doped Al_4O_4C nanowires. (d) Speculated electronic structure differences between the two phases; the possible transition level is determined based on the light emission.

future photonic elements, such as interconnections[24]. Therefore, if the waveguide ability of Si-doped Al_4O_4C nanowires is confirmed, this would present another advantage. As demonstrated in Fig. 6, a single nanowire was mechanically dispersed on a quartz substrate coated with MgF_2 film. Utilizing optical microscopy assembled with a CCD, it was then easy to drive a tapered optical fiber to help launch the laser into the nanowire via coupling with one end of the nanowire, which has been developed as a technique for manipulating lasers in the micro-domain[25–26]. Figs. 6(a–c) present optical images collected for various P_1 (input power) values for blue (473 nm), green (532 nm) and red (650 nm) lasers, respectively, for which different P_2 (output power) values were observed. To quantitatively estimate the propagation efficiency (η) through the nanowire, another tapered fiber was utilized to collect light at the emitting end, as illustrated in Fig. 6(d). Fig. 6(e) presents an optical image of the experimental configuration. The quantitative analysis shown in Figs. 6(f, g, h) indicates that there is a linear relationship between P_1 and P_2, and the efficiency (P_2/P_1) remains constant for a given wavelength, for which P_1 and P_2 were calculated based on the coupling efficiency (34.6%) between the tapered fiber and the end of the nanowire[26]. For the nanowire, the propagation efficiency of the blue light was estimated to be 80.9%, whereas values of 85.3% and 91.2% were obtained for the green and red lasers. The propagation loss primarily resulted from the light absorbing and scattering effect of the nanowire. The multi-color laser transport properties in addition to the full-color light emission behavior suggest that Si-doped Al_4O_4C 1D nanostructures can act as all-rounders in future photonic devices.

In summary, we achieved full-color light emission with a single nanowire by engineering the electronic structure using available doping technology. The CL spectrum ranges from the ultraviolet to the red region, which is attributed to CWF with a CCT of approximately 8000 K. Moreover, multi-color light guide performance was investigated for a single nanowire using the tapered light fiber coupling method. Blue, green and red lasers can propagate along the nanowire and exit at the other side. These results demonstrate the opportunity for developing new 1D inorganic nanomaterials with tunable photonic performance, which may be applicable to future photonic devices.

Methods

The Si-doped Al_4O_4C sample was prepared in a furnace, as demonstrated in our previous work[27]. A piece of an Al sheet (30 mg) was placed on a ceramic sheet with SiO powder (5 mg) on the side. Tungsten (W) foil was used as the substrate, located 50 mm away from the Al source. The ceramic sheet was pushed into a semi-closed corundum tube with the W foil toward the open side. Prior to the above process, the inner wall of the tube was scratched several times by steel tweezers to introduce Fe (catalyst) into the system. The entire assembly was placed in a furnace with the Al sheet at the center area of the graphite heater. After the chamber was pumped to ~10 Pa, the furnace was heated to 1310°C step by step over 60 minutes; the temperature was then held for 120 minutes. When the temperature increased to 350°C, CH_4 and H_2 were introduced at flow rates of 100 sccm and 5 sccm, respectively, and

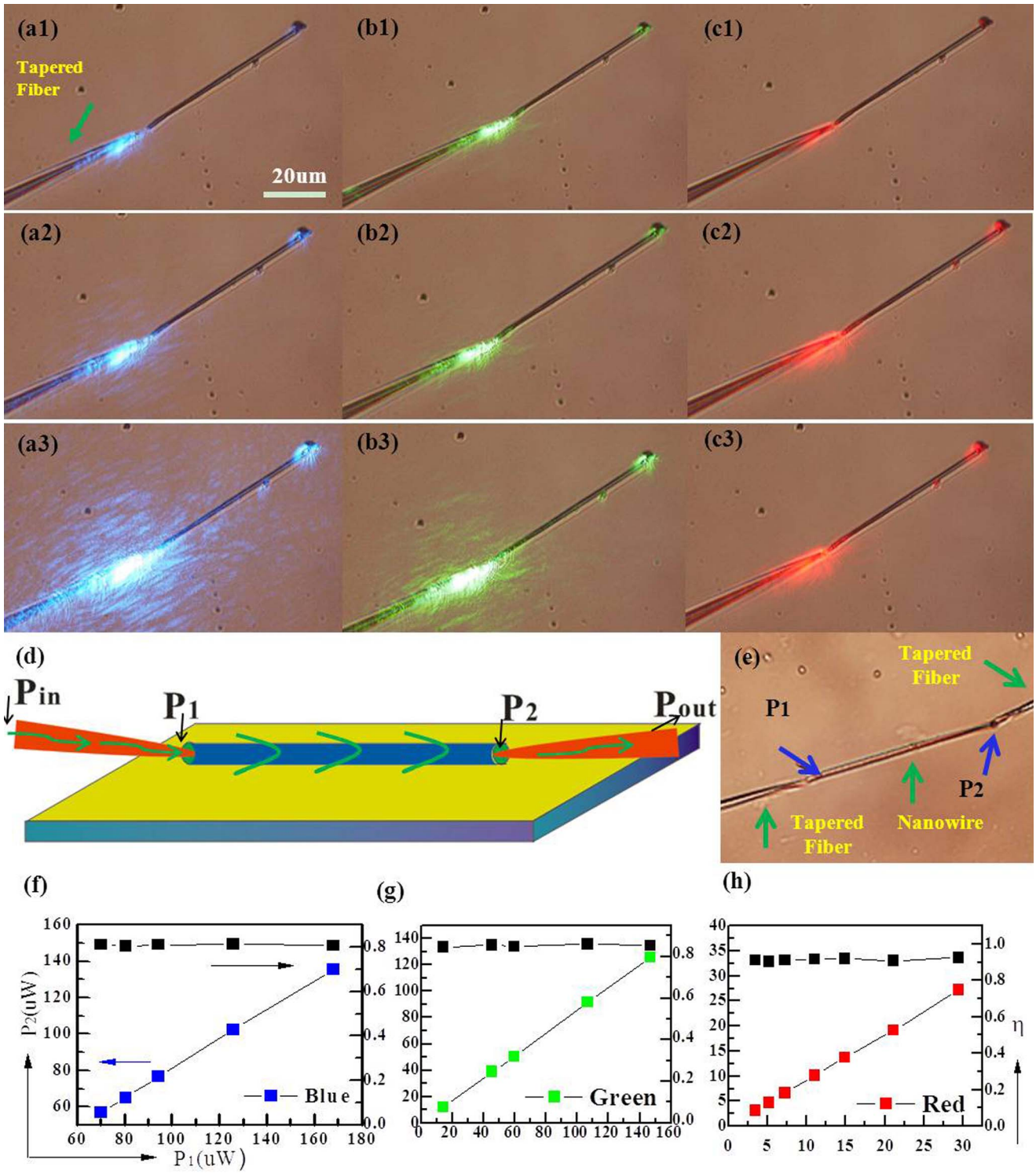

Figure 6 | (a1–a3) Optical images obtained using a 473-nm laser with various powers. (b1–b3) Optical images obtained using a 532-nm laser. (c1–c3) Optical images obtained using a 650-nm laser with various powers. (d) Illustration of the experimental configuration for the efficiency measurement, in which P_1 and P_2 represent the input and output laser power through the nanowire, respectively, and P_{in} and P_{out} represent the laser power transported across the fiber. (e) Optical image of the assembly, in which the blue arrows indicate the coupling sites between the nanowire and the tapered fibers. (f) Quantitative analysis of the propagation efficiency of the 473-nm light through the nanowire; the right axis "η" represents the transmission efficiency as recorded by the black squares. (g) Quantitative analysis of the propagation efficiency of the 532-nm laser. (h) Quantitative illustration of the propagation efficiency of the 650-nm light.

the pressure of the chamber was maintained at approximately 220 kPa (±1 kPa) until the entire process was complete. The product was located on the W substrate.

1. Zhang, C. *et al.* One-Dimensional Organic Photonic heterostructures: rational construction and spatial engineering of excitonic emission. *Adv. Mater.* **24**, 1703–1708 (2012).
2. Yang, Z. Y. *et al.* On-Nanowire spatial band gap design for white light emission. *Nano Lett.* **11**, 5085–5089 (2011).
3. Nanda, K. K., Kruis, F. E. & Fissan, H. Energy levels in embedded semiconductor nanoparticles and nanowires. *Nano Lett.* **1**, 605–611 (2001).
4. Joshi, A. *et al.* Temperature dependence of the band gap of colloidal CdSe/ZnS core/shell nanocrystals embedded into an ultraviolet curable resin. *Appl. Phys. Lett.* **89**, 131907 (2006).
5. Gong, X. *et al.* J. Multilayer polymer light-emitting diodes: white-light emission with high efficiency. *Adv. Mater.* **17**, 2053–2058 (2005).
6. Kido, J., Kimura, M. & Nagai, K. Multilayer white light-emitting organic electroluminescent device. *Science* **267**, 1332–1334 (1995).
7. Wang, Q. *et al.* Manipulating charges and excitons within a single-host system to accomplish efficiency/CRI/color-stability trade-off for high-performance OWLEDs. *Adv. Mater.* **21**, 2397–2401 (2009).
8. Li, Y. Q., Rizzo, A., Cingolani, R. & Gigli, G. Bright white-light-emitting device from ternary nanocrystal composites. *Adv. Mater.* **18**, 2545–2548 (2006).
9. Mirhosseini, R. *et al.* Improved color rendering and luminous efficacy in phosphor-converted white light-emitting diodes by use of dual-blue emitting active regions. *Opt. Express* **17**, 10807–10813 (2009).
10. Crawford, M. H. LEDs for solid-state lighting: performance challenges and recent advances. *IEEE J. Sel. Top. Quantum Electron.* **15**, 1028–1040 (2009).
11. Vanithakumari, S. C. & Nanda, K. K. A one-step method for the growth of Ga2O3-nanorod-based white-light-emitting phosphors. *Adv. Mater.* **21**, 3581–3584 (2009).
12. Bol, A. A. & Meijerink, A. Luminescence of nanocrystalline ZnS : $Pb2^{+}$. *Phys. Chem. Chem. Phys.* **3**, 2105–2112 (2001).
13. Sapra, S. *et al.* Bright white-light emission from semiconductor nanocrystals: by chance and by design. *Adv. Mater.* **19**, 569–572 (2007).
14. Bowers, M. J., McBridge, J. R. & Rosenthal, S. J. White-light emission from magic-sized cadmium selenide nanocrystals. *J. Am. Chem. Soc.* **127**, 15378–15379 (2005).
15. Rogach, A. L. *et al.* Light-emitting diodes with semiconductor nanocrystals. *Angew. Chem., Int. Ed.* **47**, 6538–6549 (2008).
16. Yan, X. H., Li, J. B. & Möhwald, H. Self-assembly of hexagonal peptide microtubes and their optical waveguiding. *Adv. Mater.* **23**, 2796–2801 (2011).
17. Barrelet, C. J., Ee, H. S., Kwon, S. H. & Park, H. G. Nonlinear Mixing in Nanowire Subwavelength Waveguides. *Nano Lett.* **11**, 3022–3025 (2011).
18. Huang, M. H. *et al.* Room-temperature ultraviolet nanowire nanolasers. *Science* **292**, 1897–1899 (2001).
19. Wang, N. W. *et al.* General strategy for nanoscopic light source fabrication. *Adv. Mater.* **23**, 2397–2939 (2011).
20. Fang, X. S. *et al.* Single-crystalline ZnS nanobelts as ultraviolet-light sensors. *Adv. Mater.* **21**, 2034–2039 (2009).
21. Li, Q. G. & Penner, R. M. Photoconductive cadmium sulfide hemicylindrical shell nanowire ensembles. *Nano Lett.* **5**, 1720–1725 (2005).
22. Sun, Y. *et al.* One-dimensional Al_4O_4C ceramics: a new type of blue light emitter. *Sci. Rep.* **3**, 1749 (2013).
23. Hui, J. F. *et al.* Ultrathin Ca-PO_4-CO_3 solid-solution nanowires: a controllable synthesis and full-color emission by rare-earth doping. *Chem. Eur. J.* **18**, 13702–13711 (2012).
24. Law, M. *et al.* Nanoribbon waveguides for subwavelength photonics integration. *Science* **305**, 1269–1273 (2004).
25. Lei, H. X., Xu, C., Zhang, Y. & Li, B. J. Bidirectional optical transportation and controllable positioning of nanoparticles using an optical nanofiber. *Nanoscale* **4**, 6707–6709 (2012).
26. Xin, H. B., Li, Y. L., Liu, X. S. & Li, B. J. Escherichia coli-based biophotonic waveguides. *Nano Lett.* 13, 3408–3413 (2013).
27. Sun, Y., Cui, H., Jin, S. X. & Wang, C. X. Eutectic solidification applied to nanofabrication: a strategy to prepare large-scale tungsten carbide nanowalls. *J. Mater. Chem.* **22**, 16566–16571 (2012).

Acknowledgments

This work was financially supported by the National Natural Science Foundation of China (No. 51125008 and No. 11274392) and the Doctoral Innovative Talents Cultivation Project at Sun Yat-sen (Zhongshan) University.

Author contributions

C.X.W. conceived and provided critical ideas for this work. Y.S. and H.X.L. performed the optical experiments. H.C. contributed to the characterization of the sample. B.J.L. and G.W.Y. analyzed the experimental results. Y.S. and C.X.W. performed the analysis and wrote the manuscript.

Additional information

Competing financial interests: The authors declare no competing financial interests.

How to cite this article: Sun, Y. *et al.* Si-Doped Ceramic Al_4O_4C Nanowires: Full-Color Emission and Optical Waveguide Behavior. *Sci. Rep.* **4**, 6833; DOI:10.1038/srep06833 (2014).